

# RSC Advances



This is an *Accepted Manuscript*, which has been through the Royal Society of Chemistry peer review process and has been accepted for publication.

*Accepted Manuscripts* are published online shortly after acceptance, before technical editing, formatting and proof reading. Using this free service, authors can make their results available to the community, in citable form, before we publish the edited article. This *Accepted Manuscript* will be replaced by the edited, formatted and paginated article as soon as this is available.

You can find more information about *Accepted Manuscripts* in the [Information for Authors](#).

Please note that technical editing may introduce minor changes to the text and/or graphics, which may alter content. The journal's standard [Terms & Conditions](#) and the [Ethical guidelines](#) still apply. In no event shall the Royal Society of Chemistry be held responsible for any errors or omissions in this *Accepted Manuscript* or any consequences arising from the use of any information it contains.

## ARTICLE

# Hooked on switch: Strain managed cooperative Jahn–Teller effect in $\text{Li}_{0.95}\text{Mn}_{2.05}\text{O}_4$ spinel

Cite this: DOI: 10.1039/x0xx00000x

Jolanta Darul,<sup>a</sup> Christian Lathe<sup>b</sup> and Paweł Piszora<sup>\*a</sup>Received 00th January 2012,  
Accepted 00th January 2012

DOI: 10.1039/x0xx00000x

www.rsc.org/

The crystal structures, phase equilibria and composition ranges of materials that form lithium-manganese spinels have been studied extensively, frequently to optimize specific properties. Here, we report about the Jahn–Teller switch between two tetragonal structures which is induced by high pressure. Heating tetragonal phases under high pressure leads to further transformation to the cubic structure. A transformation of the same type was observed upon heating of  $\text{Li}_{0.95}\text{Mn}_{2.05}\text{O}_4$  under ambient pressure, however at a milder temperature. The high-pressure high-temperature experiments were performed under pseudo-hydrostatic conditions at pressures up to 1.87 GPa and temperatures from 303 to 623 K. Furthermore, the axial ratio of tetragonal phases of  $\text{Li}_{0.95}\text{Mn}_{2.05}\text{O}_4$  is analyzed. This pressure/temperature switchable material can exhibit a wide range of novel and manipulable applications.

## Introduction

Cooperative static and dynamic orbital ordering enables developing oxides to make a switchable material that could be used in certain specific applications.<sup>1</sup> High pressure allows a controlled adjustment of structural parameters, such that their influence on the electronic and magnetic properties of materials. Physical properties such as metal-insulator transitions and superconductivity can be involved and tuned with pressure.<sup>2</sup> Recently, it has been shown that pressure can be used to operate a Jahn–Teller driven magnetic dimensionality switch, between a two-dimensional and a one-dimensional antiferromagnetic coupling.<sup>3</sup>

Classic examples of the Jahn–Teller switching between two different, closely related structure types with two distinct molecular distortions of the Jahn–Teller active cations are Tutton salts of copper,  $\text{A}_2[\text{Cu}(\text{H}_2\text{O})_6][(\text{S},\text{Se})\text{O}_4]_2$  ( $\text{A} = \text{K}^+, \text{Rb}^+, \text{Cs}^+, \text{NH}_4^+, \text{Ti}^+$ ). Propensity for undergoing a phase transition and structural switching depends on the chemical strain induced with the hydrogen-bonding interactions and monovalent cations balance.<sup>4</sup> Moreover, in the deuterated ammonium copper Tutton salt, the long axis of Jahn–Teller distortion changes direction, which causes a switch between two crystal forms, and the switch driving agent is the pressure induced strain.<sup>5</sup> There are many examples of Jahn–Teller switching in manganese doped perovskites. Thermally and electrically induced switching in the  $\text{LaGa}_{1-x}\text{Mn}_x\text{O}_3$  systems between high resistance and low-resistance states has been explained in terms of thermo-induced local phase transition resulting in the oxidation of  $\text{Mn}^{3+}$  ions and local removal of the Jahn–Teller distortion.<sup>6</sup>  $\text{Mn}^{3+}$  ions are Jahn–Teller ions, which cause specific distortions to the crystal lattice. The oxidation of  $\text{Mn}^{3+}$  to  $\text{Mn}^{4+}$  would result in both removal of such a distortion and increase in the number of carriers. Manipulating Jahn–Teller distortions under pressure has been widely reviewed for  $\text{Cu}^{2+}$  as a central ion.<sup>7</sup> In the coordination systems with diverse

coordination atoms, such as  $\text{CuF}_2(\text{H}_2\text{O})_2$  (pyrazine), each trans-coordinated ligand provides an additional degree of freedom to the Jahn–Teller effect. In this type of compounds small perturbations of the metal-ligand environment can be enough to rotate the Jahn–Teller axis and radically modify the material properties. Pressure may act as a switching agent, especially for the organic framework with relatively high compressibility. Rotation of the Jahn–Teller axis with pressure in the  $\text{CuF}_2(\text{H}_2\text{O})_2$  (pyrazine) structure switches between quasi-two-dimensional to a quasi-one-dimensional antiferromagnetic phase.<sup>3,8</sup> Moreover, Cu(II) citrate dimer reveals pressure-induced coordination change that leads to piezochromism.<sup>9</sup>

Pressure can also affect lithium-manganese spinels, which are important for energy storage and for purpose-engineered materials. Spinel manganites (such as  $\text{LiMn}_2\text{O}_4$ ,  $\text{Li}_4\text{Mn}_5\text{O}_{12}$  and similar materials) are very interesting and complex systems, with interesting correlation between electric transport and magnetic properties and crystal-lattice behaviour. The progenitor of this group of materials,  $\text{LiMn}_2\text{O}_4$ , contains in the unit cell 32 oxide anions, arranged in a cubic close-packed lattice, 8  $\text{Li}^+$  ions on 1/8 of 64 tetrahedral holes and a 1:1 mixture of  $\text{Mn}^{3+}$  and  $\text{Mn}^{4+}$  ions distributed over 1/2 of 32 octahedral sites. Properties of these materials depend strongly on the composition, in particular, on point defects and on the doping concentration, which induces changes in the relative content of  $\text{Mn}^{4+}/\text{Mn}^{3+}$  ions.<sup>10–12</sup> Pressure and temperature can be used to obtain lithium-manganese oxide with orthorhombic structure (*Pnma*) referred to as the postspinel phase.<sup>13</sup> The high-pressure postspinel structure comprises irregular hexagonal 1D channel which implies the diffusive motion of  $\text{Li}^+$  ions in  $\text{Li}_{0.92}\text{Mn}_2\text{O}_4$ , desirable for positive electrode material.<sup>14,15</sup> Calculations within the first-principles density functional theory (DFT) show details of the spinel-to-post-spinel phase transformation, and provides kinetic explanation of the stability of the postspinel HP/HT phase under ambient conditions.<sup>16</sup>

Deformation of the tetragonally deformed spinels exposed to high pressure is usually reduced, as manifested by the axial ratio reduction and the atomic positions getting closer to the ideal cubic spinel value. Quite different structural changes are observed for the Jahn–Teller ions in the structure, when we go out of pure hydrostaticity, and semi-hydrostatic or even non-hydrostatic compression is applied. Even small deviation from hydrostatic conditions can facilitate the pressure-induced phase transition and in turn leads both to new deformation of the nearest neighbourhood of  $\text{Mn}^{3+}$  ions and a cooperative Jahn–Teller deformation. The transition pressures of  $\text{LiMn}_2\text{O}_4$  in different pressure transmitting media were reported to be below 0.5 GPa<sup>17</sup> and 1.2 GPa<sup>18</sup> for silicon oil, 0.2 GPa for boron nitride,<sup>18</sup> 1.2 GPa for NaCl,<sup>18</sup> 4.36 GPa<sup>19</sup> and 11.0 GPa<sup>20</sup> for methanol-ethanol. These results and survival after the pressure relaxation of the high-pressure artefacts in the samples compressed in nonhydrostatic conditions, indicate that deviatoric stress rather than absolute pressure plays the key role in this phase transition.<sup>20,21</sup>

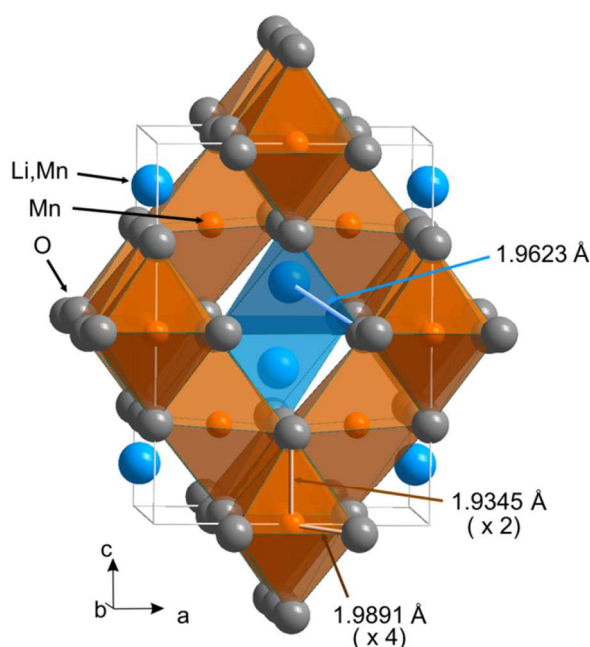


**Fig. 1** Crystal structure of  $\text{Li}_{0.95}\text{Mn}_{2.05}\text{O}_4$  under ambient conditions, space group  $Ia_1/amd$ ,  $c/a\sqrt{2} = 0.97809$ .

It is also possible to control the Jahn–Teller deformation, and as a result physicochemical properties of materials, with epitaxial strain in thin films.<sup>22</sup> The effect of the substrate on the film can be divided into two kinds of strain: the planar strains along the film plane  $xy$  and the axial strain along the growth direction  $z$ . Since the substrate is typically cubic or pseudocubic, the planar strain is almost isotropic. Epitaxial strain is the reason why the cubic structure of  $\text{Mn}_3\text{O}_4$  has been observed instead of the tetragonal one in the thin film grown on  $\text{MgO}$  as a substrate.<sup>23</sup> However, for  $\text{MgAl}_2\text{O}_4$  as a substrate, the lattice mismatch is minimized and growth of the tetragonal  $\text{Mn}_3\text{O}_4$  phase has been observed with the  $c$  axis elongated in the direction perpendicular to the substrate surface.<sup>24</sup> Thus, the Jahn–Teller deformation type control can be performed not only with temperature and pressure, as we present, but potentially also with the use of epitaxial strain.

In this article we would like to call attention to the interesting effect of reorientation of the cooperative Jahn–Teller effect in the material of particular stoichiometry and obtained in a specific way. We would like to highlight the unusual structural property of  $\text{Li}_{0.95}\text{Mn}_{2.05}\text{O}_4$  that is its ability to switch between three types of crystal structure: two of them with the cooperative Jahn–Teller effect of different types of tetragonal deformation, and one cubic without manifested cooperative Jahn–Teller effect.

## Experimental

The  $\text{Li}_{0.95}\text{Mn}_{2.05}\text{O}_4$  spinel sample was obtained from the appropriate amounts of thoroughly mixed powders of  $\alpha\text{-Mn}_2\text{O}_3$  and  $\text{Li}_2\text{CO}_3$  (99.0% Merck), by successive thermal treatment in air at 973 K and, after grinding, at 1073 K for 4 h, in air. Finally, the specimen was quenched rapidly in the solid  $\text{CO}_2$ . The precursor ( $\alpha\text{-Mn}_2\text{O}_3$ ) was prepared by precipitation of Mn-hydroxide from  $\text{Mn}^{2+}$  nitrate solution ( $\text{Mn}(\text{NO}_3)_2 \cdot 6\text{H}_2\text{O}$ , 99.0% Merck) with sodium hydroxide (98.8% POCH). Washed and dried at room temperature, it was dehydrated for 2 h at 523 K and then successively at 673, 773, and 873 K for 4 h in air. The crystalline single-phase precursor displayed the bixbyite ( $Ia3$ ) structure. The tetragonally-distorted spinel structure of the final sample was confirmed by an X-ray diffraction pattern recorded on an X-ray diffractometer Bruker D8 Advance in the Bragg-Brentano configuration equipped with a Johansson monochromator ( $\lambda\text{Cu K}\alpha_1 = 1.5406\text{\AA}$ ) and using a strip detector LynxEye. Refinement with the Rietveld method was performed for the pattern collected in the angular range  $15 - 120^\circ 2\theta$  using the Jana2006 program.<sup>25</sup>

TG measurements were run by means of a Setsys 1200 (Setaram) system with the heating rate of 10 K/min in air. Chemical composition of spinel samples was analysed by inductively coupled plasma-optical emission spectroscopy (Varian ICP-OES VISTA-MPX).

$\text{Li}_{0.95}\text{Mn}_{2.05}\text{O}_4$  was studied in HP/HT conditions in the pressure range from ambient to 1.87 GPa by means of energy-dispersive X-ray diffraction (EDXRD) at beamline F2.1 at Desy/HASYLAB with typical collection time of  $\sim 6$  min per pattern. The diffraction patterns were recorded using a CANBERRA semiconductor (germanium) detector with a resolution of 153 and 500 eV for energies of 5.9 and 122 keV, respectively (the total average resolution  $\delta d/d \approx 1\%$ ), with the diffraction angle fixed at  $3.84062^\circ$ . The sample was mounted on a large-anvil diffraction press, MAX80, in a cylindrical sample container made from hexagonal boron nitride (hBN) inserted into a graphite resistance heater in a cube fabricated from a mixture of boron and epoxy resin. To achieve the quasi-hydrostatic compression conditions the studied polycrystalline material was mixed (1:3) with hexagonal boron nitride. The accuracy of pressure determination was evaluated to be  $\pm 0.05$  GPa. With increasing temperature we observed a fluctuation in pressure; however, it did not exceed the accuracy of pressure determination. The temperature was measured by the NiCr–Ni thermocouple with a stability of  $\pm 2$  K.

Under the pressure of 1.87 GPa, and in the temperature range 303 – 623 K, the semi-isobaric measurements were performed. The diffraction from sodium chloride sample which was mounted separately in the sample compartment, was used to calibrate the pressure according to Decker EOS.<sup>26</sup> To monitor the change in lattice parameters with pressure we fitted diffraction patterns with the Le Bail method. There was no need for special adjustments of experimental patterns for

fluorescence because in the analysed energy range there were no fluorescence maxima of any present elements. Diffraction patterns were fitted with the Jana2006 program<sup>25</sup> which enabled refinement with anisotropic strain broadening with meaningful tensor parameters.<sup>27</sup> Prior to the Le Bail fitting, XRD patterns were converted into conventional pseudo angle-dispersive data (CuK $\alpha_1$  radiation). This whole diffraction pattern profile fitting allows determination of the lattice parameters and it works especially well with overlapping of peaks because in this method the intensity is defined on the basis of the multiplicity of the intensities that contribute to a particular peak.

Moreover, the study was performed in high-temperature conditions under ambient pressure by the synchrotron angle-dispersive X-ray diffraction (ADXRD) method. The X-ray diffraction studies at varied temperatures were carried out with a powder diffractometer at the B2 beamline (HASYLAB/DESY). The powder sample was mounted in a quartz capillary which rotated during the experiment inside a capillary furnace (STOE). A curved on-site readable imaging plate detector was applied for the data collection. The powder diffraction patterns were recorded in the range  $5^\circ - 60^\circ$   $2\theta$ . The wavelength was adjusted to 0.70998 Å. For the patterns collected in the high-temperature experiment, the Rietveld refinement was performed using the Jana2006 program.<sup>25</sup>

## Results and discussion

ICP-EOS analysis confirmed the nominal cation ratio in the prepared lithium-manganese oxide. The Li/Mn ratio was of  $0.465 \pm 0.004$  (confidence interval of the mean value was calculated for 6 repetition, standard deviation  $\sigma = 0.0043$  and statistical confidence  $P = 95\%$ ), whereas for the 'ideal'  $\text{LiMn}_2\text{O}_4$  and  $\text{Li}_{0.95}\text{Mn}_{2.05}\text{O}_4$  the Li/Mn ratio is 0.500 and 0.463, respectively. Thermogravimetric analysis (ESI Figure S1) indicated that the evident mass loss upon heating occurs only if temperature exceeds 1150 K, therefore, at the synthesis temperature of 1073 K thermal dissociation and formation of anionic vacancies could be neglected. Thus, the combination of ICP and thermogravimetric analysis revealed that the chemical composition of the sample agrees well with the nominal composition and is indeed  $\text{Li}_{0.95}\text{Mn}_{2.05}\text{O}_4$ .

The applied combination of sintering at high temperatures followed by a very rapid quenching process enabled producing a spinel material that has been impossible to obtain earlier.<sup>28,29</sup> Samples of the Li/Mn ratio smaller than  $\frac{1}{2}$  are multi-phased if they are not quenched after the sintering step.<sup>30</sup>

For the lithium-manganese oxide of the chosen stoichiometry, the quenching does not preserve the high temperature crystal structure, but enables the synthesis of a new material of intriguing structure and unusual hitherto-unknown properties.  $\text{Mn}^{3+}$  ion exist in the spinel structure of  $\text{Li}_{0.95}\text{Mn}_{2.05}\text{O}_4$  in both tetrahedral and octahedral coordination.<sup>31</sup> The  $\text{Mn}^{3+}$  cations occupy partially the four-coordinate sites of the spinel structure where removal of the degeneracy of the  $d^4$  ground state results in flattening of the  $\text{MnO}_4$  tetrahedron, as observed in  $\text{CuCr}_2\text{O}_4$  with  $\text{Cu}^{2+}$  as a tetrahedrally coordinated Jahn–Teller ion.<sup>32</sup> The local structure deformation, induced by the Jahn–Teller  $\text{Mn}^{3+}$  ions introduced on the tetrahedral sites, competes with the Jahn–Teller elongation of the  $\text{Mn}^{3+}\text{O}_6$  octahedra, typically observed in manganese-containing spinels (e.g. in  $\text{Mn}_3\text{O}_4$ ). However, even the small amount of  $\text{Mn}^{3+}$  on tetrahedral sites is able to induce a kind of chemical strain and forces one of two energetically indistinguishable Jahn–Teller deformations on the  $\text{Mn}^{3+}\text{O}_6$  octahedra. Finally, a quite unusual

tetragonal spinel of space group  $I4_1/amd$  (space group no. 141) and  $c/a' < 1$  was obtained as confirmed by the Rietveld refinement of the laboratory ADXRD data (ESI Figure S3). Figure 1 shows the unit cell of the  $\text{Li}_{0.95}\text{Mn}_{2.05}\text{O}_4$  spinel with tetrahedra occupied by Li and Mn atoms and the 'flattened' octahedra with two short Mn–O distances, practically parallel to the  $c$  axis, and four long Mn–O distances almost in the (110) plane. (for structural data see Electronic Supplementary Information Tables S1 and S2). Although the Le Bail profile fitting and the Rietveld refinement were performed with  $I4_1/amd$  space group, a straightforward illustration of the tetragonal distortion of the spinel structure requires the use of  $F4_1/ddm$  space group as an alternative description of the  $I4_1/amd$  space group. We assume a notation for unit cell parameters in  $I4_1/amd$  space group as  $a$  and  $c$ , and for the face-centred pseudocubic cell ( $F4_1/ddm$ ) we express  $\sqrt{2}a = a'$  and  $c = c'$ . Our earlier experience with quenching of the  $\text{Li}_x\text{Mn}_{3-x}\text{O}_4$  lithium-deficient spinels allowed us to choose the nominal stoichiometry of  $\text{Li}_{0.95}\text{Mn}_{2.05}\text{O}_4$  as the most promising for the synthesis of the tetragonal spinel of  $c/a' < 1$ , although this tetragonal deformation has been observed in a major phase for samples of compositions between  $\text{Li}_{0.94}\text{Mn}_{2.06}\text{O}_4$  and  $\text{Li}_{0.97}\text{Mn}_{2.03}\text{O}_4$ .<sup>31</sup>

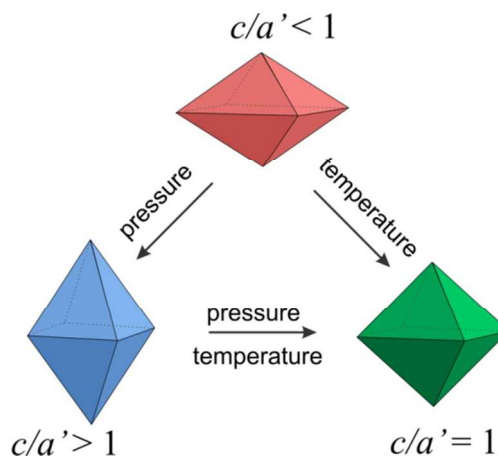


Fig. 2 Schematic diagram of phase transitions in  $\text{Li}_{0.95}\text{Mn}_{2.05}\text{O}_4$

It should be stressed that the tetragonal deformation of the spinel structure for this stoichiometry is different from that of the high-temperature tetragonal spinel, observed *in-situ* for  $\text{LiMn}_2\text{O}_4$  (tetragonal,  $I4_1/amd$   $c/a' > 1$ ),<sup>33</sup> and also it does not correspond to the low-temperature structure of  $\text{LiMn}_2\text{O}_4$  (orthorhombic,  $Fddd$ )<sup>34</sup> (See Electronic Supplementary Information, Fig. S2). Eventually, the crystal structure deformation of  $\text{Li}_{0.95}\text{Mn}_{2.05}\text{O}_4$  is also different from that of the single crystal tetragonal spinel  $(\text{Li}_{0.91}\text{Mn}_{0.09})\text{Mn}_2\text{O}_4$  synthesized by the flux method (tetragonal,  $I4_1/amd$   $c/a' > 1$ ).<sup>35</sup>

The Synchrotron EDXRD patterns were collected under various pressures up to 1.87 GPa, and then, for a fixed pressure at various temperatures up to 623 K (ESI Figure S4). The Le Bail method enabled refinement of the unit cell parameters (Tables 1 and 2), the profile parameters, and the peak intensities to match the measured powder diffraction patterns collected in each high pressure/high temperature (HP/HT) condition. The Le Bail refinement was successfully used to show the phase transitions in HP/HT experiments. Models of two tetragonal spinels ( $I4_1/amd$ ) for  $c/a' < 1$  and  $c/a' > 1$  were sufficient to obtain a good fitting results in the pressure region from 0.15 GPa to 1.87 GPa (representative results are presented in Figure



**Table 1** Unit-cell parameters of crystal phases under various pressure and quality parameters of profile refinement with Le Bail technique

P [GPa]	Tetragonal $c/a' < 1$		Tetragonal $c/a' > 1$		$R_p$ [%]	$R_{wp}$ [%]
	$a$ [Å]	$c$ [Å]	$a$ [Å]	$c$ [Å]		
0	5.8911(8)	8.160(2)	—	—	4.66	9.12
0.15	5.8876(5)	8.126(2)	5.746(1)	8.549(3)	4.26	6.10
0.27	5.8840(8)	8.121(2)	5.741(2)	8.569(4)	4.27	6.65
0.46	5.887(1)	8.106(3)	5.734(2)	8.574(3)	3.99	6.17
0.96	5.897(1)	8.066(4)	5.7216(9)	8.591(2)	5.24	7.69
1.39	5.888(1)	8.046(4)	5.7093(7)	8.587(2)	4.65	6.12
1.80	5.876(2)	8.041(6)	5.697(2)	8.586(4)	5.71	7.84

3a). The initial models were assumed on the basis of the Rietveld refinement for this sample under ambient conditions for  $c/a' < 1$  (for the structural data see Electronic Supplementary Information) and on the basis of literature data for  $c/a' > 1$ .<sup>33</sup> Moreover, the Le Bail profile fitting of the synchrotron EDXRD patterns collected at temperatures higher than 373 K and under high pressure required input of a model of the cubic spinel phase, with the crystal structure analogous to that of  $\text{LiMn}_2\text{O}_4$ . Representative results of the Le Bail fitting for HP/HT measurements are presented in Figure 3aC,D) and the obtained unit cell parameters are collected in Table 2.

Correlation of Jahn–Teller local deformations in the spinel structure containing ions at degenerate electronic ground states, such as  $\text{Mn}^{3+}$ , leads to the cooperative Jahn–Teller effect. Using pressure and temperature we can change the degree of deformation and switch between two different stages of the Jahn–Teller deformation. It is also possible to transform the tetragonal structure with the cooperative Jahn–Teller effect to the cubic structure with the statistically disordered distortion (Figure 2). Figure 3b shows the representative part of the raw EDXRD patterns (corresponding to cubic spinel 311 and 222 lines) for  $\text{Li}_{0.95}\text{Mn}_{2.05}\text{O}_4$  spinel as a function of pressure up to 1.87 GPa and further under a fixed pressure as a function of temperature. Vanishing of the reflections derived from the initial tetragonal phase with  $c/a' < 1$  is coupled with increasing intensities of the ones corresponding to the new tetragonal phase, of the axial ratio  $c/a' > 1$  (ESI Figure S4). This phase transition was also confirmed by the Le Bail whole pattern profile fitting with the pseudo angle-dispersive patterns, beforehand converted from the energy-dispersive data (Figure 3a). Under the pressure of 1.87 GPa, we found evidence for the coexistence of two tetragonal phases in a ratio of about 1:1 (Figure 3aB).

In the Jahn–Teller distorted spinel phase, the ordering of the tetragonally distorted octahedra is caused by the interaction of local distortions through the phonon field, and is a temperature-dependent interaction of electronic properties and phonon branches. With increasing temperature, the correlations of local distortions weaken, and at a critical temperature the phase transition to the distortion-disordered phase takes place. The

presence of the tetragonal phase of  $c/a' > 1$  remains discernible at 573 K, whereas heating to 623 K leads to formation of a pure cubic structure (Figure 3aD). Therefore, the observed phase transitions induce anomalies to the elastic crystalline properties and consequently they induce substantial changes in the electronic structure (change in a splitting of the degenerate energy levels), also in the vicinity of the tetragonal-to-cubic phase transition all the crystalline electronic parameters also can exhibit appreciable anomalies.

With increasing pressure, the tetragonal phases showed an increasing or decreasing  $c/a'$  ratio for the tetragonal  $c/a' > 1$  or  $c/a' < 1$  phase, respectively. The pressure-dependence of the lattice parameters ratio provides quantitative evidence of the reorientation of the Jahn–Teller distortion of  $\text{Mn}^{3+}\text{O}_6$ , where  $\text{Mn}^{3+}$  is located at the centre of this octahedron with each of the  $\text{Mn}^{3+}$ -oxygen bonds directed approximately along the  $a$ - $b$  diagonal and the  $c$  cell edge of the tetragonal unit cell. Figure 4 shows that there is a difference between the modes by which strain is accommodated in the high-pressure tetragonal phase ( $c/a' > 1$ ) compared to the primary tetragonal phase ( $c/a' < 1$ ). An interesting feature is that the axial ratio of the tetragonal phase with  $c/a' < 1$  decreases only to about 0.967 under ~1 GPa and does not change significantly on further compression. Athwart, the axial ratio of the pressure-induced phase (with  $c/a' > 1$ ) increases monotonically with pressure, although this tendency is in contradiction to the rule of the tetragonally distorted spinels response to pressure according to which pressure diminishes the distortion or even does not affect the axial ratio.<sup>36,37</sup> However, results presented are consistent with the earlier observations for  $\text{LiMn}_2\text{O}_4$ <sup>20,21</sup> which suggests a specific mechanism for the lithium-manganese samples compressed beyond the limit of hydrostaticity. The  $c/a'$  ratio reached under 2.87 GPa is consistent with that reported for the tetragonal phase obtained by quenching  $\text{LiMn}_2\text{O}_4$  from 1193 K. Only slightly smaller  $c/a'$  ratio, 1.062, has been reported for the single crystal obtained by the flux method. This indicates that the elongation of the spinel unit cell obtained in our HP experiment corresponds to those of the known structures of  $\text{MnO}_6$  octahedra elongated in the  $c$  direction.

**Table 2** Unit-cell parameters of crystal phases under the pressure of 1.87 GPa at various temperatures and quality parameters of profile refinement with the LeBail technique

T [K]	Tetragonal $c/a' < 1$		Tetragonal $c/a' > 1$		Cubic $a$ [Å]	$R_p$ [%]	$R_{wp}$ [%]
	$a$ [Å]	$c$ [Å]	$a$ [Å]	$c$ [Å]			
303	5.876(2)	8.041(6)	5.697(2)	8.586(4)	—	5.71	7.84
323	5.880(1)	8.056(3)	5.699(2)	8.591(3)	—	3.51	5.13
373	5.877(1)	8.027(3)	5.715(1)	8.568(4)	—	5.77	7.43
423	5.896(2)	8.040(4)	5.731(1)	8.555(4)	8.241(2)	4.76	6.36
473	—	—	5.727(1)	8.533(5)	8.235(2)	4.49	6.23
523	—	—	5.742(1)	8.512(6)	8.242(2)	4.49	6.21
573	—	—	5.760(1)	8.469(6)	8.251(2)	4.88	6.54

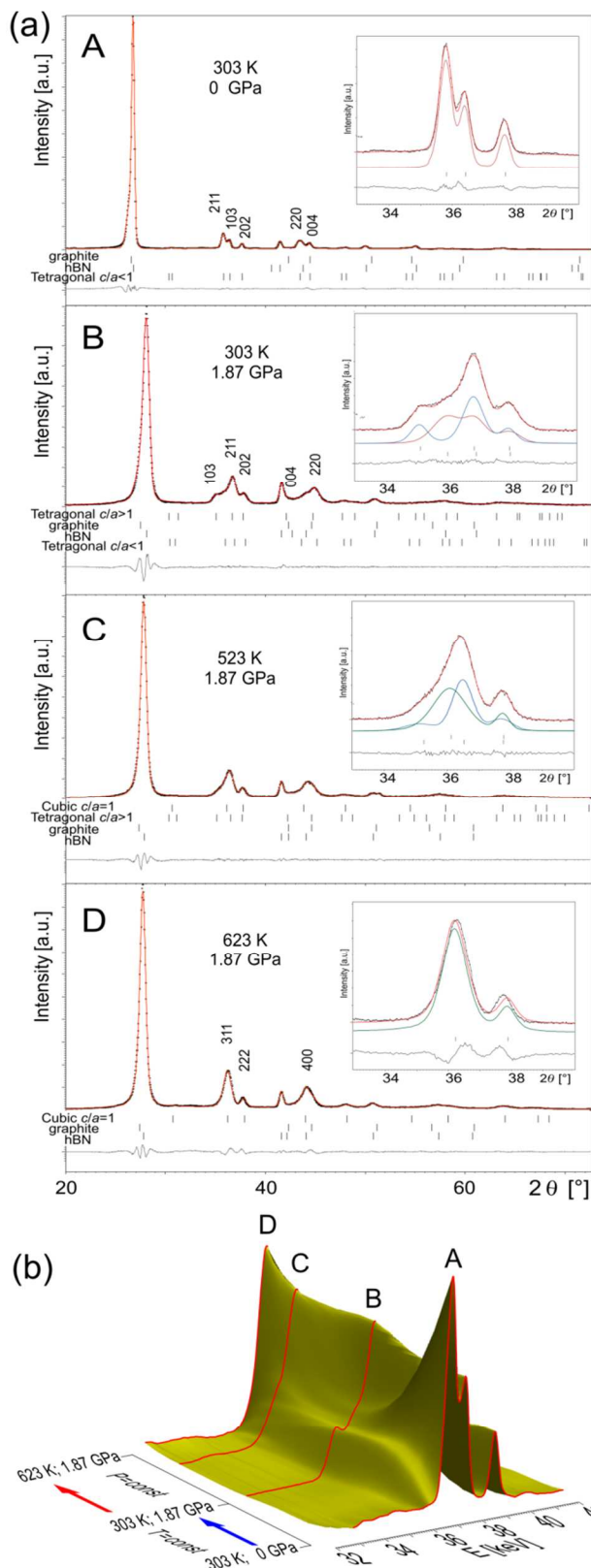


**Fig. 3** (a) LeBail refinement results. For the sake of clarity, not all peaks in the patterns were indexed. Indices in part A – tetragonal spinel structure ( $I4_1/amd$ ) with  $c/a < 1$ ; B – tetragonal spinel structure ( $I4_1/amd$ ) with  $c/a > 1$ ; D – cubic spinel ( $Fd\bar{3}m$ ). The vertical bars indicate the positions of Bragg peaks. (b) representation of the raw energy-dispersive X-ray diffraction profiles of  $\text{Li}_{0.95}\text{Mn}_{2.05}\text{O}_4$  as a function of pressure and temperature.

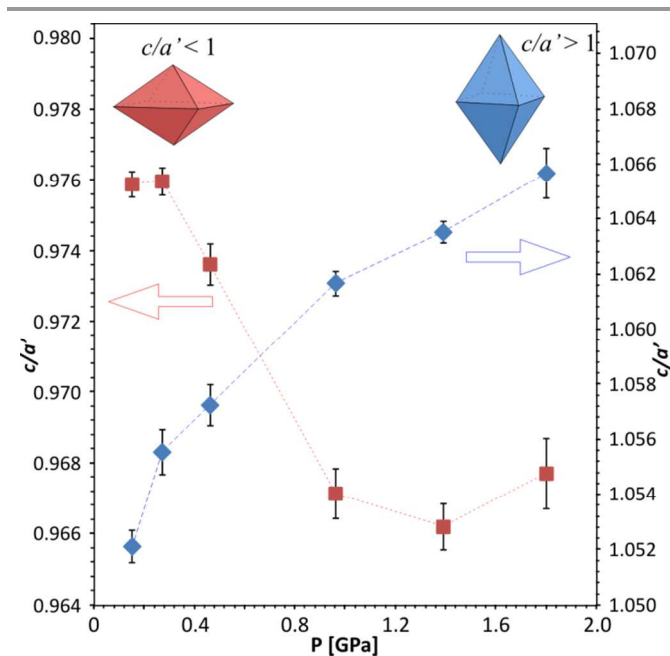


**Fig. 4** The  $c/a'$  ratio of the lattice parameters for two tetragonal phases: the initial one with  $c/a' < 1$  (squares) and the high pressure phase with  $c/a' > 1$  (diamonds).

The observed modulation of the axial ratio with pressure is expected to be of interest in thin layers technology, because a similar modulation of the axial ratio can be obtained in thin layers through an appropriate choice of substrate and the layer thickness, and films can be grown with various aspect ratios. The epitaxial stress has been successfully applied in modification of physical properties of  $\text{LaCoO}_3$ . The lattice mismatch in epitaxial thin films of  $\text{LaCoO}_3$  on  $\text{SrTiO}_3$  produces

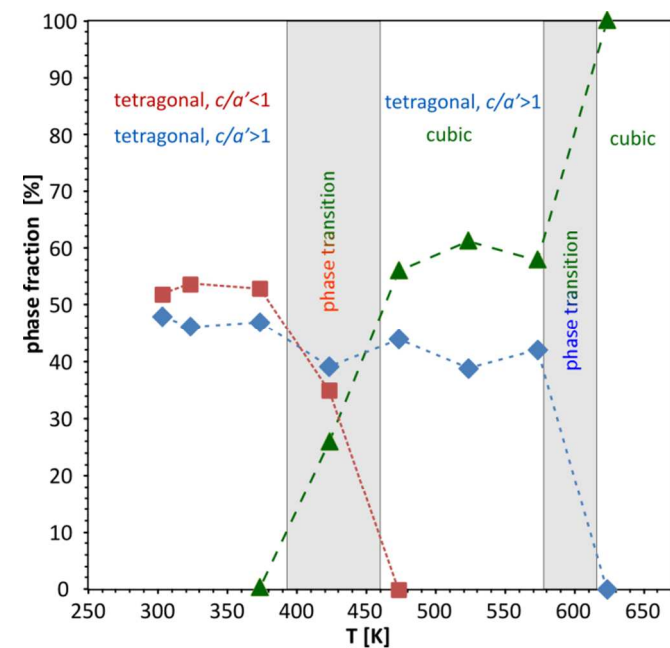


**Fig. 5** The phase composition of the sample under the pressure of 1.8 GPa as a function of temperature obtained from the EDXRD experiment. Squares: % of the tetragonal phase with  $c/a' < 1$ ; diamonds: % of the tetragonal phase with  $c/a' > 1$ ; triangles: % of the cubic phase.

**Table 3** Unit-cell parameters of crystal phases under the ambient pressure at various temperatures and quality parameters of Rietveld refinement

T [K]	Tetragonal $c/a' < 1$		Cubic $a$ [Å]	Rp [%]	Rwp [%]
	$a$ [Å]	$c$ [Å]			
297	5.874(1)	8.1189(15)		5.57	7.11
373	5.873(2)	8.194(3)		5.4	6.84
393	5.850(2)	8.233(3)	8.258(3)	5.33	6.78
413			8.265(1)	5.49	6.98

a tensile strain, making these films one of the few FM-insulators known among transition-metal oxides.<sup>38</sup>

The evolution of the phase composition of the  $\text{Li}_{0.95}\text{Mn}_{2.05}\text{O}_4$  spinel with temperature for  $P = \text{const} = 1.87$  GPa is illustrated in Figure 5. The first temperature-induced phase transition appears at about 423 K and is a transformation of the tetragonal phase with  $c/a' < 1$  to the cubic phase. This temperature-induced suppression of the cooperative Jahn–Teller effect was also observed in the ADXRD high temperature experiment for  $\text{Li}_{0.95}\text{Mn}_{2.05}\text{O}_4$ , where Rietveld refinement results reveal 393 K as the temperature of the tetragonal-to-cubic phase transition (Figure 7). Thus, under the pressure of 1.87 GPa this phase transition is shifted of about 30 K in the direction of higher temperature, compared to that which was observed under ambient pressure.

The percentage of the second tetragonal phase induced with high pressure, with  $c/a' > 1$ , remains almost unchanged up to 573 K; finally, at 623 K this phase abruptly disappears. In this temperature region the second phase transition is observed which could be attributed to statistical disorder of the elongated  $\text{Mn}^{3+}$  octahedra within the octahedral sublattice of the spinel structure.

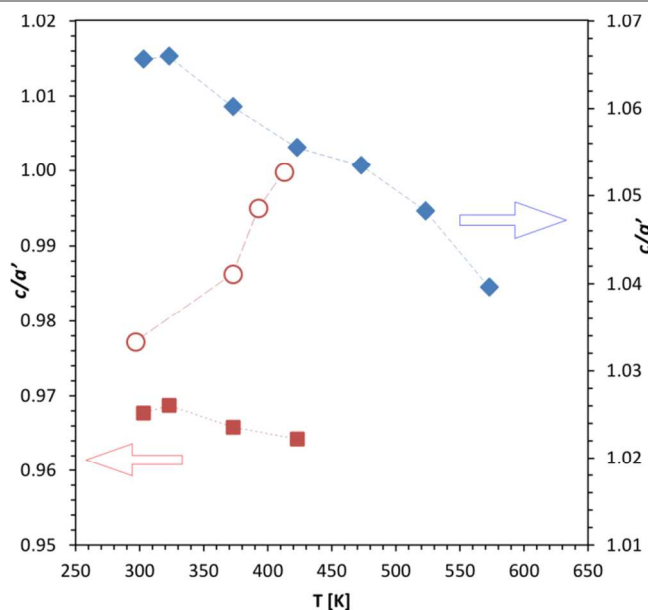


**Fig. 6** The  $c/a'$  ratio of the lattice parameters for tetragonal phases as a function of temperature: with  $c/a' < 1$  under 1.87 GPa (squares); with  $c/a' > 1$  under 1.87 GPa (diamonds); with  $c/a' < 1$  under ambient pressure (open circles).

Axial ratio,  $c/a'$ , remains almost unchanged with increasing temperature for the tetragonal phase of  $c/a' < 1$  under 1.87 GPa (Figure 6). However, for the tetragonal phase of  $c/a' > 1$  the axial ratio decreases gradually from 1.0657 at 303 K to 1.0397 at 573 K. Similar suppression of the cooperative Jahn–Teller effect is manifested in the ADXRD high temperature experiment for the tetragonal phase of  $c/a' < 1$  (ESI Figure S5),

which in Figure 6 can be observed as an increase in  $c/a'$  ratio. The results of Rietveld refinement for ADXRD patterns collected at 298, 393 and 413 K are shown in Figure 7 and in Table 3. The tetragonal-to-cubic phase transition was induced by heating. At about 393 K both tetragonal ( $c/a' < 1$ ) and cubic phase were observed, whereas at 413 K only cubic phase occurred. Inflection of the  $c/a'$  ratio as a function of temperature at about 373 K (Figure 6) gently suggests an additional structural phenomenon. An additional phase transition is possible and can be driven by a charge ordering such as observed in  $\text{Fe}_3\text{O}_4$  and in  $\text{LiMn}_2\text{O}_4$ ,<sup>34,39</sup> however, to resolve it the high resolution measurements are necessary.

Thus, it is possible to obtain the pressure- and temperature-induced Jahn–Teller switch based on the spinel framework with variable-valence metal ion and precisely fitted synthesis path. It might be a new route to look for new applications of this spinel materials. Further investigation based on the influence of Jahn–Teller effect on crystallochemistry of this group of materials is still in progress. These high-pressure and high-temperature phase transformations are important as they provide a potential pathway to obtaining new materials with desirable properties. Furthermore, we can expect that this approach to novel switchable materials is not limited to only one material with specific stoichiometry.

## Conclusions

In the present contribution we have added new information to the knowledge on lithium-manganese spinels by determining the structural properties of  $\text{Li}_{0.95}\text{Mn}_{2.05}\text{O}_4$  characterized by their Jahn–Teller instability. Pseudo-hydrostatic compression leads to small perturbations in the Jahn–Teller ion environment and can be sufficient to switch the Jahn–Teller deformation type and radically modify properties of the spinel material. High pressure application is indicated as an ideal method of achieving such a unique phenomenon. Heating under the pressure of 1.87 GPa transforms both tetragonal phases,  $c/a' < 1$  and  $c/a' > 1$ , to the phase of cubic structure with suppressed cooperative Jahn–Teller effect. Under ambient pressure, heating of the tetragonal  $\text{Li}_{0.95}\text{Mn}_{2.05}\text{O}_4$  spinel ( $c/a' < 1$ ) also leads to formation of the cubic structure, however, at a milder temperature.

## Acknowledgements

Some of the research has been carried out at the beamline F2.1 of the light source DORIS III, at DESY, a member of the Helmholtz Association (HGF). The research leading to these results has received funding from the European Community's Seventh Framework Programme (FP7/2007-2013) under grant agreement n° 312284.

## Notes and references

<sup>a</sup> Department of Materials Chemistry, Faculty of Chemistry, Adam Mickiewicz University, Umultowska 89b, 61-614 Poznań, Poland.

<sup>b</sup> Helmholtz Centre Potsdam, GFZ German Research Centre for Geosciences, Telegrafenberg 14473 Potsdam, Germany.

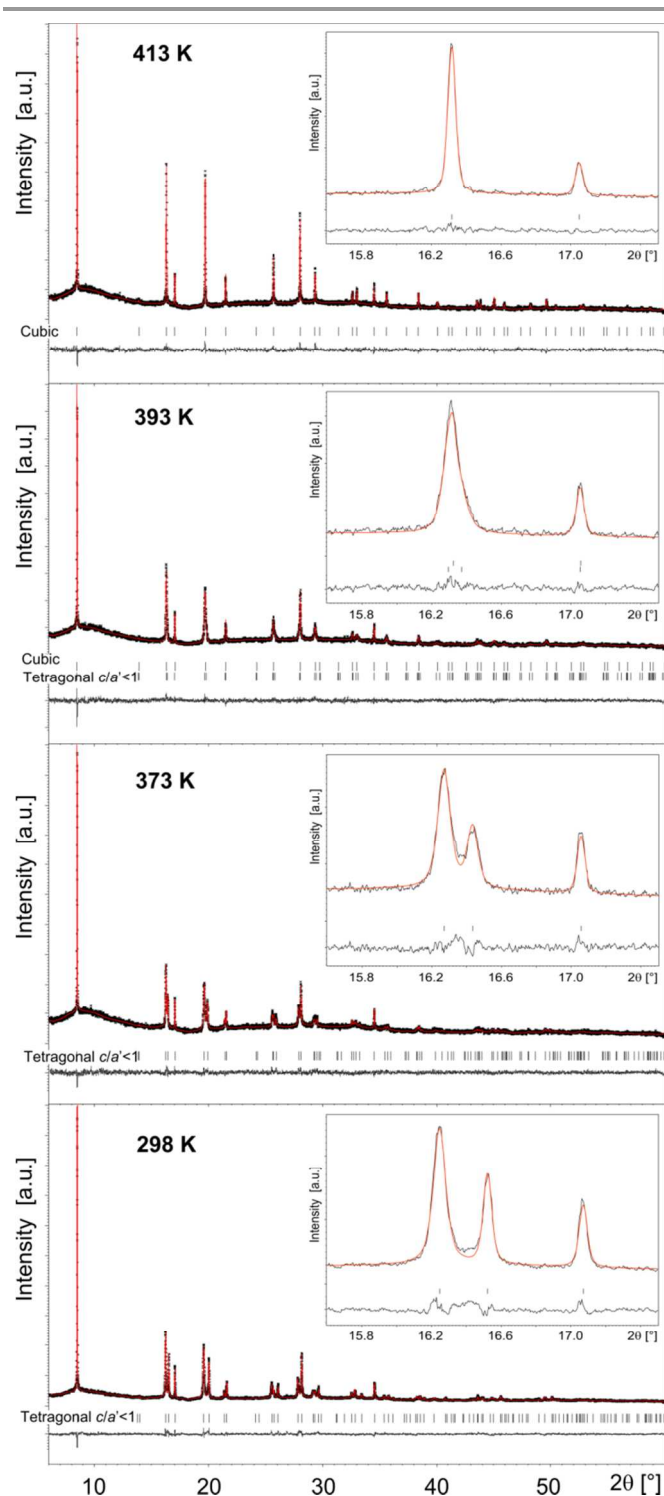


**Fig. 7** Observed, calculated and difference profile from Rietveld refinement of the synchrotron ADXRD patterns obtained for  $\text{Li}_{0.95}\text{Mn}_{2.05}\text{O}_4$  at various temperatures under ambient pressure. The vertical bars indicate the positions of Bragg peaks.

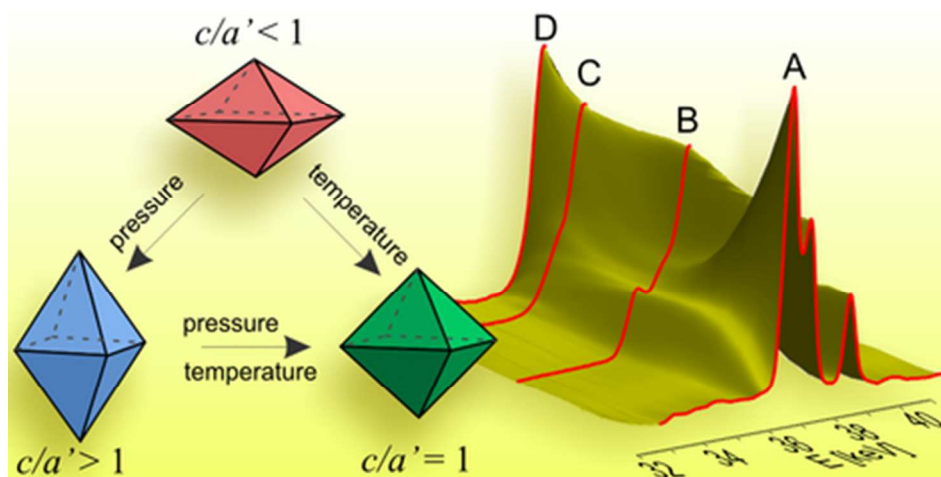
Electronic Supplementary Information (ESI) available: Thermogravimetric curve; Comparison of the experimental XRD pattern with the patterns calculated for typical structures of lithium-manganese oxides; Results of the Rietveld refinement of the  $\text{Li}_{0.95}\text{Mn}_{2.05}\text{O}_4$  pattern collected under ambient conditions; EDXRD patterns obtained in HP/HT

experiment; ADXRD patterns obtained at various temperatures under ambient pressure. See DOI: 10.1039/b000000x/

- 1 J. B. Goodenough, *Chem. Mater.*, 2014, **26**, 820–829.
- 2 V. D. Blank and E. I. Estrin, *Phase Transitions in Solids Under High Pressure*. CRC Press, 2013.
- 3 S. Ghannadzadeh, J. S. Möller, P. A. Goddard, T. Lancaster, F. Xiao, S. J. Blundell, A. Maisuradze, R. Khasanov, J. L. Manson, S. W. Tozer, D. Graf and J. A. Schluter, *Phys. Rev. B*, 2013, **87**, 241102.
- 4 C. J. Simmons, H. Stratemeier, M. A. Hitchman and M. J. Riley, *Inorg. Chem.*, 2013, **52**, 10481–10499.
- 5 L. R. Falvello, *J. Chem. Soc., Dalton Trans.*, 1997, **23**, 4463–4476.
- 6 N. Noginova, J. McClure, E. Etheridge, V. I. Gavrilenko and D. Novikov, *J. Phys. D: Appl. Phys.*, 2008, **41**, 055411.
- 7 M. A. Halcrow, *Chem. Soc. Rev.*, 2013, **42**, 1784–1795.
- 8 A. Prescimone, C. Morien, D. Allan, J. A. Schluter, S. W. Tozer, J. L. Manson, S. Parsons, E. K. Brechin and S. Hill, *Angew. Chem. Int. Ed.*, 2012, **51**, 7490–7494.
- 9 K. W. Galloway, S. A. Moggach, P. Parois, A. R. Lennie, J. E. Warren, E. K. Brechin, R. D. Peacock, R. Valiente, J. González, F. Rodríguez, S. Parsons and M. Murrie, *CrystEngComm*, 2010, **12**, 2516–2519.
- 10 K. Hoang, *J. Mater. Chem. A*, 2014, DOI: 10.1039/C4TA04116J
- 11 M. Kopeck, J. R. Dygas, F. Krok, A. Mauger, F. Gendron and C. M. Julien, *J. Phys. Chem. Solids*, 2008, **69**, 955–966.
- 12 D. Liu, W. Zhu, J. Trottier, C. Gagnon, F. Barray, A. Guerfi, A. Mauger, H. Groult, C. M. Julien, J. B. Goodenough and K. Zaghib, *RSC Adv.*, 2014, **4**, 154–167.
- 13 K. Yamaura, Q. Huang, L. Zhang, K. Takada, Y. Baba, T. Nagai, Y. Matsui, K. Kosuda and E. Takayama-Muromachi, *J. Am. Chem. Soc.*, 2006, **128**, 9448–9456.
- 14 Y. Ikeda, J. Sugiyama, O. Ofer, M. Månsson, H. Sakurai, E. Takayama-Muromachi, E. J. Ansaldo, J. H. Brewer and K. H. Chow, *J. Phys.: Conf. Ser.*, 2010, **225**, 012017.
- 15 M. Mamiya, K. Kataoka, J. Akimoto, S. Kikuchi, Y. Terajima and K. Tokiwa, *J. Power Sources*, 2013, **244**, 561–564.
- 16 C. Ling and F. Mizuno, *Chem. Mater.*, 2013, **25**, 3062–3071.
- 17 A. Paolone, A. Sacchetti, P. Postorino, R. Cantelli, A. Congeduti, G. Rousse and C. Masquelier, *Solid State Ionics*, 2005, **176**, 635–639.
- 18 P. Piszora, *Z. Kristallogr. Suppl.*, 2007, **26**, 387–392.
- 19 J. Darul, W. Nowicki and P. Piszora, *J. Phys. Chem. C*, 2012, **116**, 17872–17879.
- 20 Y. Lin, Y. Yang, H. Ma, Y. Cui and W. L. Mao, *J. Phys. Chem. C*, 2011, **115**, 9844–9849.
- 21 P. Piszora, *Solid State Phenom.*, 2007, **130**, 69–72.
- 22 A. M. Haghiri-Gosnet and J. P. Renard, *J. Phys. D: Appl. Phys.*, 2003, **36**, R127.
- 23 O. Y. Gorbunov, I. E. Graboy, V. A. Amelichev, A. A. Bosak, A. R. Kaul, B. Güttler, V. L. Svetchnikov and H. W. Zandbergen, *Solid State Commun.*, 2002, **124**, 15–20.
- 24 L. Ren, M. Yang, W. Zhou, S. Wu and S. Li, *J. Phys. Chem. C*, 2014, **118**, 243–249.
- 25 V. Petricek, M. Dusek and L. Palatinus, Jana2006. The crystallographic computing system. Institute of Physics, Praha, Czech Republic, 2006.



- 26 D. L. Decker, W. A. Bassett, L. Merrill, H. T. Hall and J. D. Barnett, *J. Phys. Chem. Ref. Data*, 1972, **1**, 773-836.
- 27 P. W. Stephens, *J. Appl. Cryst.*, 1999, **32**, 281-289
- 28 T. R. Hinklin, J. Azurdia, M. Kim, J. C. Marchal, S. Kumar and R. M. Laine, *Adv. Mater.*, 2008, **20**, 1373-1375.
- 29 S. Yeo, S. Guha and S. W. Cheong, *J. Phys.: Condens. Mat.*, 2009, **21**, 125402.
- 30 P. Piszora, *J. Alloy. Compd.*, 2005, **401**, 34-40.
- 31 P. Piszora, *Chem. Mater.*, 2006, **18**, 4802-4807.
- 32 B. J. Kennedy and Q. Zhou, *J. Solid State Chem.*, 2008, **181**, 2227-2230.
- 33 R. Kanno, A. Kondo, M. Yonemura, R. Gover, Y. Kawamoto, M. Tabuchi and G. Rousse, *J. Power Sources*, 1999, **81**, 542-546.
- 34 J. Rodriguez-Carvajal, G. Rousse, C. Masquelier and M. Hervieu, *Phys. Rev. Lett.*, 1998, **81**, 4660-4663.
- 35 H. Björk, H. Dabkowska, J. E. Greedan, T. Gustafsson and J. O. Thomas, *Acta Crystallogr. Sect. C*, 2001, **57**, 331-332.
- 36 J. Darul, C. Lathe and P. Piszora, *J. Phys. Chem. C*, 2013, **117**, 23487-23494.
- 37 S. Åsbrink, A. Waśkowska, L. Gerward, J. S. Olsen and E. Talik, *Phys. Rev. B*, 1999, **60**, 12651.
- 38 F. Rivadulla, Z. Bi, E. Bauer, B. Rivas-Murias, J. M. Vila-Funqueiriño and Q. Jia, *Chem. Mater.*, 2012, **25**, 55-58.
- 39 M. S. Senn, J. P. Wright and J. P. Attfield, *Nature*, 2012, **481**, 173-176.



Compression and heating of  $\text{Li}_{0.95}\text{Mn}_{2.05}\text{O}_4$  induce a unique three way switch. We demonstrate the possibility of tuning of the structural properties and induction of phase transitions by changing external pressure and temperature and hence by changing the lattice strain.

39x19mm (300 x 300 DPI)